

See discussions, stats, and author profiles for this publication at: <https://www.researchgate.net/publication/277892562>

Influence of Fluorine Substitution on the Unusual Solid-State [2 + 2] Photo-Cycloaddition Reaction between an Olefin and an Aromatic Ring

ARTICLE in CRYSTAL GROWTH & DESIGN · JUNE 2015

Impact Factor: 4.89 · DOI: 10.1021/acs.cgd.5b00664

READS

18

5 AUTHORS, INCLUDING:



Hui Yang

National University of Singapore

7 PUBLICATIONS 127 CITATIONS

SEE PROFILE

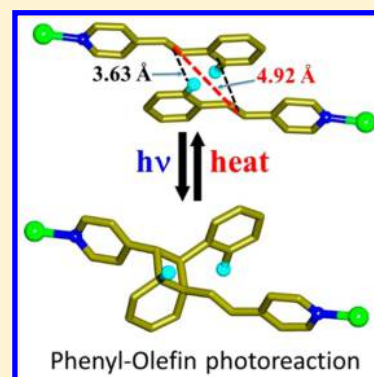
Influence of Fluorine Substitution on the Unusual Solid-State [2 + 2] Photo-Cycloaddition Reaction between an Olefin and an Aromatic Ring

Raghavender Medishetty, Zhaozhi Bai, Hui Yang, Ming Wah Wong,* and Jagadese J. Vittal*

Department of Chemistry, National University of Singapore, 3, Science Drive 3, 117543, Singapore

S Supporting Information

ABSTRACT: Solid-state [2 + 2] photo-cycloaddition reactions observed so far were exclusively between a pair of olefin bonds. Usually when the phenyl–olefin bonds have been closely aligned, they were found to be either photoinert or sliding of molecules takes place for [2 + 2] cycloaddition reaction between olefins in the solid state, although intramolecular phenyl–olefin reactions are well-known in solution. In the crystal structure of $[\text{Zn}_2(\text{ptol})_4(4\text{spy})_2]$ (ptol = *para*-toluate), the neighboring 4-styrylpyridine (4spy) ligands are organized in a head-to-tail manner. On one side of the complex in the crystal structure, the olefin bonds in the 4spy pairs are perfectly aligned to undergo cycloaddition reaction, but on the other side, the olefin bond pairs are slightly offset and found to be photoinert at 223 K forming only a dimer in single crystals. The sliding of 4spy groups has been restricted by the steric hindrance of the adjacent methyl group of the ptol ligands. A similar packing of 2-fluoro-4'-styrylpyridine (2F-4spy) pairs was found in $[\text{Zn}_2(\text{ptol})_4(2\text{F-4spy})_2]$. Again, normal cycloaddition reaction occurs on one side of the 2F-4spy ligand pairs, whereas the second offset 2F-4spy ligand pairs undergo a rare [2 + 2] cycloaddition reaction between the fluorophenyl group and olefin bond resulting in the formation of a one-dimensional coordination polymers containing a bicyclic product in a quantitative yield. The bicyclic ring in the photoproduct can be thermally cleaved back to olefin and phenyl groups. These observations have been confirmed by single-crystal X-ray crystallography, ^1H NMR, and ^{19}F NMR studies. Density functional theory calculations were performed to elucidate the nature of the interactions between the fluorophenyl and olefin groups. The greater reduction of aromaticity of 2F-4spy in the excited singlet state compared to the 4spy system may explain the observed reactivity difference between the two systems. The improved reactivity in 2F-4spy may also be attributed to the fact that the olefin–phenyl distance is shorter in 2F-4spy than in 4spy (3.63 versus 3.69 Å). This solid state phenyl–olefin photodimerization helps to pave the way for making new bicyclic derivatives.

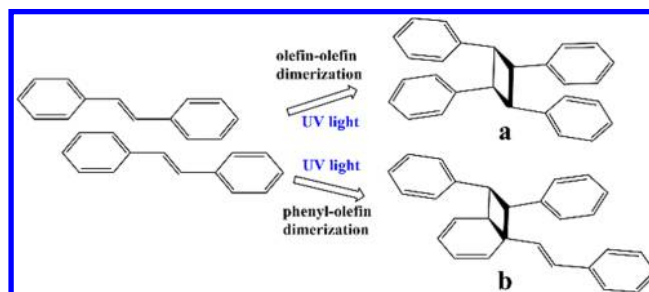


■ INTRODUCTION

The solid-state [2 + 2] cycloaddition reaction dates back to the work of Lieberman in 1889 on the photodimerization of cinnamic acid.¹ The formation of α -truxillic and β -truxinic acids from two types of cinnamic acid crystals was subsequently interpreted as crystal lattice controlled reaction by Bernstein and Quimby in 1943.² Later, Schmidt and his co-workers correlated the structures of the cinnamic acids and several other enone derivatives with the steric configurations of their photoproducts and introduced the topochemical principles.^{3–5} Since then several hundreds of photo-cycloaddition reactions have been reported to take place exclusively between a pair of olefin bonds.^{6–9} In a number of cases where Schmidt's topochemical criteria were not met, the olefin pairs were either found to be photostable or underwent sliding/pedal motion to meet the criteria in the solid state as shown in Scheme 1.^{10–13}

A simple Cambridge Structural Database search for the intermolecular alignment between olefin and phenyl bonds within 3.5–4.2 Å distance criterion generates more than 100 000 hits.¹⁴ Despite this, solid-state photo-cycloaddition reaction between olefin bond and phenyl ring has rarely been reported, where it has been found to occur up to only 66%, as

Scheme 1. (a) Normal [2 + 2] Cycloaddition between a Pair of Olefin Bonds after Sliding of Molecules. (b) Intramolecular Photodimerization between Phenyl and Olefin Bonds Usually Observed in Solution



characterized by NMR spectroscopy.¹⁵ In contrast, intramolecular cyclization between phenyl group and olefin bond have been extensively studied in solution (Scheme 1b).^{16–18}

Received: May 13, 2015

Published: June 2, 2015



During the course of our investigation we stumbled upon this interesting asymmetric photo-cycloaddition between a fluorenyl ring and an olefin bond driven by the solid-state packing of the molecules. Although the phenyl ring and an olefin bond are closely aligned between the neighboring 4-styrylpyridine (4spy) ligands of a Zn(II) complex, it was almost photostable. The reaction readily occurs under UV light when 4spy was replaced by 2-fluoro-4'-styrylpyridine (2F-4spy) in the Zn(II) complex in a single-crystal-to-single-crystal (SCSC) manner and further supported by ^{19}F and ^1H NMR spectral data. We have shown that in addition to the alignment of phenyl–olefin bonds, fluorine substitution influences the quantitative dimerization reaction in the solid state. The details are discussed below.

EXPERIMENTAL SECTION

Materials and Methods. All the chemicals and solvents were of reagent grade and purchased from different commercial resources and were used without further purification. 4spy and 2F-4spy were synthesized according to the literature.^{19,20} Powder X-ray diffraction (PXRD) data were recorded on a D5005 Siemens X-ray diffractometer with graphite monochromatized Cu K α radiation ($\lambda = 1.54056 \text{ \AA}$) at room temperature (298 K). NMR spectra were recorded on a 300 or 400 MHz FT-NMR spectrometer with residual solvent as the reference in DMSO- d_6 solution for ^1H NMR and trifluoroacetic acid as a standard for ^{19}F -NMR chemical shifts. Thermogravimetric analysis (TGA) was performed under nitrogen atmosphere with a heating rate of $5 \text{ }^\circ\text{C min}^{-1}$ on a TA Instruments SDT-2960. The C, H, N analyses were carried using Elementar Vario Micro Cube instrument at the Elemental Analysis Lab, CMMAC, Department of Chemistry, National University of Singapore.

All the UV irradiation experiments were conducted in a LUZCHEM UV reactor. In the case of crystalline powders, the ground single crystals were packed in between the glass slides placed in the UV reactor. These glass slides were flipped back at regular intervals of time to maintain the uniform exposure of UV irradiation. The SCSC transformation of **1** to **2** was performed on the diffractometer at 223 K using Asahi spectra MAX 150, and in the case of **4** to **5**, all the small crystals or platy crystals cracked into pieces under UV irradiation. However, the big block-shaped crystals survived the photoreaction after exposing the crystals for 3 h UV using an Asahi spectra MAX 150 instrument.^{21–24}

Synthesis of $[\text{Zn}_2(\text{ptol})_4(4\text{spy})_2]$ **1.** Pale yellow block-shaped single crystals were obtained from the slow evaporation of the aqueous methanol solution of $\text{Zn}(\text{OAc})_2 \cdot 2\text{H}_2\text{O}$ (11 mg, 0.05 mmol), *p*-toluic acid (13.6 mg, 0.1 mmol), and 4spy (9 mg, 0.05 mmol) and the addition of three drops of 0.75 M NaOH. The crystals were dried at room temperature (yield: 16 mg (62%)). ^1H NMR (DMSO- d_6 , 300 MHz, 298 K): δ 8.55 ppm (s, 4H, pyridyl protons of 4spy), 7.83 ppm (d, $J = 8.1 \text{ Hz}$, 8H, ptol protons), 7.2–7.7 ppm (m, 18H, aromatic protons of 4spy), 7.21 ppm (d, 8H, $J = 7.8 \text{ Hz}$, *p*-toluate protons), 2.34 ppm (s, 12H, methyl protons of *p*-tol). The elemental analysis (%) Calculated for $\text{C}_{29}\text{H}_{25}\text{NO}_4\text{Zn}$ (516.90): C, 67.38; H, 4.87; N, 2.71. Found: C, 67.00; H, 4.45; N, 2.64. IR (KBr pellet, cm^{-1}) 1610 (s), 1564 (s), 1509 (m), 1413 (s), 1212 (m), 1177 (s), 1030 (m), 972 (s), 860 (m), 818 (s), 762 (s), 688 (s), 625 (m), 543 (s).

Synthesis of $[\text{Zn}_4(\text{ptol})_8(\text{rctt-ppcb})(4\text{spy})_2]$ **2.** Single crystals of **2** were obtained by keeping the single crystals of **1** under UV light for 1–2 h at $-50 \text{ }^\circ\text{C}$. ^1H NMR (DMSO- d_6 , 300 MHz, 298 K): δ 8.55 ppm (s, 4H, pyridyl protons of 4spy), δ 8.33 ppm (d, 4H, $J = 7.1 \text{ Hz}$, pyridyl protons of *rctt-ppcb*), 7.83 ppm (d, 16H, $J = 7.1 \text{ Hz}$, ptol protons), 7.0–7.8 ppm (m, 32H, aromatic protons of *rctt-ppcb* and 4spy), 7.21 ppm (d, 16H, $J = 7.8 \text{ Hz}$, *p*-toluate protons), 4.61 (s, 4H, cyclobutane proton, *rctt-ppcb*), 2.34 ppm (s, 24H, methyl protons of *p*-tol).

Synthesis of $[\text{Zn}_2(\text{ptol})_4(\text{rctt-ppcb})]$ **3.** Single crystals of **1** were ground finely and packed between the slides and exposed to UV for more than 80 h. ^1H NMR (DMSO- d_6 , 300 MHz, 298 K): δ 8.33 ppm

(4H, pyridyl protons of *rctt-ppcb*), 7.83 ppm (d, 8H, $J = 7.4 \text{ Hz}$, ptol protons), 7.0–7.4 ppm (m, 14H, aromatic protons of *rctt-ppcb*), 7.22 ppm (d, 8H, $J = 7.8 \text{ Hz}$, *p*-toluate protons), 4.61 (s, 4H, cyclobutane proton, *rctt-ppcb*), 2.34 ppm (s, 12H, methyl protons of *p*-tol). IR data. 1700 (m), 1610 (s), 1561 (s), 1508 (m), 1414 (s), 1224 (m), 1176 (m), 1112 (m), 1070 (m), 1032 (m), 972 (m), 850 (m), 825 (m), 766 (s), 700 (s), 625 (m), 544, 473 (m), 438 (m).

If the single crystals of **1** were irradiated under UV light for 120 h, the ^1H NMR has more peaks in addition to **2** along with shift in pyridyl peak from δ 8.55 ppm could not be completely assigned. See Figure S13 in Supporting Information.

Synthesis of $[\text{Zn}_2(\text{ptol})_4(2\text{F-4spy})_2]$ **4.** Colorless block single crystals were obtained from the slow evaporation of the aqueous ethanolic solution of $\text{Zn}(\text{OAc})_2 \cdot 2\text{H}_2\text{O}$ (11 mg, 0.05 mmol), *p*-toluic acid (13.6 mg, 0.1 mmol), and 2F-4spy (10 mg, 0.05 mmol) and the addition of three drops of 0.75 M NaOH. The crystals were dried at room temperature (yield: 15 mg (56%)). The elemental analysis (%) Calculated for $\text{C}_{29}\text{H}_{24}\text{FNO}_4\text{Zn}$ (534.89): C, 65.12; H, 4.52; N, 2.62. Found: C, 65.00; H, 4.24; N, 2.64. ^1H NMR (DMSO- d_6 , 300 MHz, 298 K): δ 8.58 ppm (d, 4H, $J = 7.3 \text{ Hz}$, pyridyl protons of 2F-4spy), 7.84 ppm (d, 4H, $J = 8.1 \text{ Hz}$, pyridyl protons of 2F-4spy), 7.2–7.7 ppm (m, 12H, aromatic protons of 2F-4spy), 7.21 ppm (d, 8H, $J = 7.9 \text{ Hz}$, *p*-toluate protons), 2.34 ppm (s, 12H, methyl protons of *p*-tol). IR (KBr pellet, cm^{-1}) 1609 (s), 1562 (s), 1505 (s), 1411 (s), 1223 (m), 1178 (m), 1110, 1028 (m), 975, 855 (m), 818 (m), 762 (s), 692 (m), 629 (m), 554, 518, 477, 425.

Synthesis of $[\text{Zn}_2(\text{ptol})_4(2\text{F-ppcb})_{0.5}(\text{L1F})_{0.5}]$ **5.** Compound **4** was subjected to UV-irradiation for 2 h. ^1H NMR (DMSO- d_6 , 300 MHz, 298 K): δ 8.58 ppm (d, 2H, $J = 7.5 \text{ Hz}$, pyridyl protons of **L1F**), 8.48 ppm (d, 2H, $J = 7.6 \text{ Hz}$, pyridyl protons of **L1F**), 8.35 ppm (d, 4H, $J = 7.5 \text{ Hz}$, pyridyl protons of *rctt-2F-ppcb*), 7.83 (d, 8H, $J = 9.2 \text{ Hz}$, aromatic protons of *p*-toluate), 7.2 ppm (d, 8H, $J = 9.1 \text{ Hz}$, aromatic protons of ptol), 6.9–7.7 ppm (m, 8H, aromatic protons of *rctt-2F-ppcb*, 6H, **L1F**), 6.2–6.6, 5.2–5.5, 3.66 (m, 8H, olefinic protons of **L1F**), 4.72 ppm (s, 4H, cyclobutane protons of *rctt-2F-ppcb*), 2.34 (s, 12H, methyl protons of *p*-toluate). IR (KBr pellet, cm^{-1}): 1600 (s), 1563 (m), 1510, 1414 (s), 1230, 1178, 1110, 1071, 1034, 851, 764 (s), 694, 627, 567(m), 476, 444.

X-ray Crystallography. Crystal data of all these crystals were collected on a Bruker APEX diffractometer attached with a CCD detector and graphite-monochromated Mo K α radiation ($\lambda = 0.71073 \text{ \AA}$) using a sealed tube. Absorption corrections were made with the program SADABS,²⁵ and the crystallographic package SHELXTL^{26,27} was used for all calculations. Crystallographic data and structural refinements for **1**, **2**, **4**, and **5** are listed in Supplementary Table 1. CCDC 1007520–1007523 (**1**, **2**, **4**, and **5**) contains the supplementary crystallographic data of this paper.

RESULTS AND DISCUSSION

Pale yellow single crystals of $[\text{Zn}_2(\text{ptol})_4(4\text{spy})_2]$ (**1**) (ptol = *para*-toluate) were obtained by slow evaporation of the aqueous ethanol solution of $\text{Zn}(\text{OAc})_2$, *p*-toluic acid, and 4spy in a 1:2:1 molar ratio with three drops of 0.75 M NaOH solution. This compound crystallized in the monoclinic space group $P2_1/c$ with $Z = 4$, and the asymmetric unit contains a formula unit. Each Zn(II) atom is bridged by two ptol ligands and asymmetrically chelated by a ptol as shown in Figure 1. Hence, each Zn(II) atom adopts a distorted square pyramidal geometry with a pyridyl nitrogen atom occupying the apical position. Both the chelated ptol ligands are almost parallel but slip-stacked. The coordination sphere observed here is very rare and different from the well-known paddle-wheel structure. A CSD search showed only one example for this geometry among various discrete metal complexes.²⁸

Crystallographic inversion centers are present on the both sides of the molecule close to the middle of the neighboring 4spy ligands, resulting in the neighboring 4spy molecules to

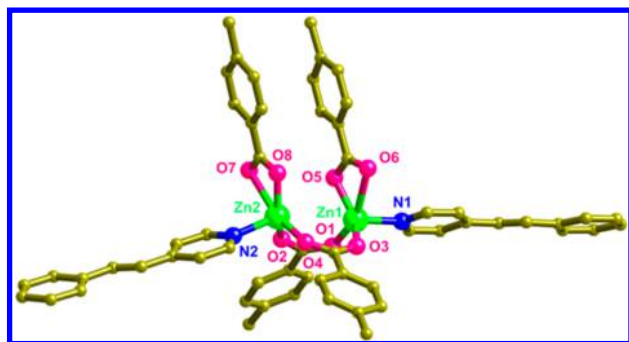


Figure 1. Ball and stick model of compound **1**. The hydrogen atoms are omitted for clarity.

align in a head-to-tail fashion. Because of the asymmetrical building unit, different types of alignments of 4spy pairs occur on both sides of **1**. The pyridyl and phenyl groups of the 4spy ligands bonded to Zn1 atoms are aligned face to face with a center-to-center separation of 3.77 Å, while the well-aligned olefin groups are separated by 3.73 Å, which is well within the Schmidt's topochemical criteria.^{4,5,29} Hence, this C=C pair is expected to be photoreactive under UV light and likely to furnish the anticipated cyclobutane derivative quantitatively. On the contrary, the 4spy ligand pairs bonded to the Zn2 atoms are also aligned parallel but slip-stacked. The middle of each C=C bond is closer to the center of the neighboring phenyl ring (3.55 Å). This olefin pair is expected to be photoinert unless the ligands slide during the photo reaction under UV light.^{4,5,7}

The single crystal of **1** after data collection was irradiated under UV light for 1 h at 223 K at the diffractometer. The X-ray crystallography reveals the formation of a new compound, $[\text{Zn}_4(\text{ptol})_8(\text{rctt-ppcb})(4\text{spy})_2]$, **2** (where *rctt-ppcb* = *regio-cis, trans, trans*-1,3-bis(4'-pyridyl)-2,4-bis(phenyl)cyclobutane) as shown in Figure 2.

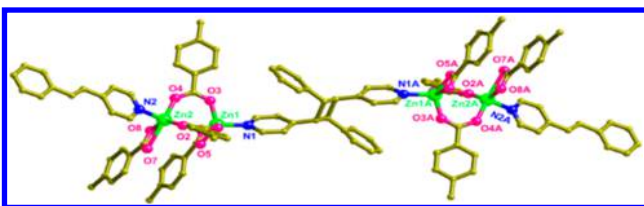


Figure 2. Ball and stick model of compound **2** and showing cyclobutane ring. Symmetry code (A): $2 - x, 2 - y, 2 - z$. The hydrogen atoms are not shown.

The Zn(II) complex **2** has a crystallographic inversion center at the center of the cyclobutane ring. Overall, the packing in **2** is very similar to that of **1**, and the center of the adjacent phenyl ring is closer to the middle of olefin bond by 3.55 Å. The methyl groups from the neighboring ptol ligands from the *b*-direction mutually hinder sliding of the adjacent 4spy ligands. However, grinding of **1** or **2** and exposure to UV light yielded quantitative photoproduct, $[\text{Zn}_2(\text{ptol})_4(\text{rctt-ppcb})]$ (**3**), as determined from ¹H NMR spectral data recorded after dissolving in DMSO-*d*₆ (see Figure S14 in Supporting Information). It is likely that the mechanical grinding changed the crystal packing, and hence the alignment of the adjacent 4spy ligands to account for the complete disappearance of olefin protons upon UV exposure. Further, the powder X-ray diffraction (PXRD) pattern of the powdered **2** is different from the simulated pattern of the single crystal data of **2**, lending

support to our conclusion (Figure S19 in Supporting Information).

On the contrary, a number of new peaks started appearing in the ¹H NMR spectrum of the single crystals of **1** irradiated for 120 h at room temperature indicating that some other side reaction has also taken place in addition to normal [2 + 2] cycloaddition reaction. However, the intensities of these new peaks are too low and masked by the intense peaks of *rctt-ppcb* (Figure S13, Supporting Information). These additional chemical shifts could arise from the reaction of C=C bond with other parts of the adjacent 4spy ligand, isomerization or cyclization. Attempts have been made to synthesize an isostructural compound with different substituents on 4spy ligand and fluoro substitution on the *ortho* position of the phenyl group, namely, *trans*-2-fluoro-4'-styrylpyridine (2F-4spy) resulted in very similar packing.

Colorless block shaped single crystals of $[\text{Zn}_2(\text{ptol})_4(2\text{F-4spy})_2]$ (**4**) were synthesized by a procedure similar to **1**, and the crystal structure is also isotypical to **1**. However, one of the Zn(II) has slightly different coordination sphere. Both Zn(II) atoms are bridged by two ptol ligands and chelated by a ptol anion. But an oxygen atom (O5) of one of the chelated ptol ligands is also bridging the other Zn(II) atom (Zn2–O5, 2.504 Å) as shown in Figure 3. This is also reflected in the twisting

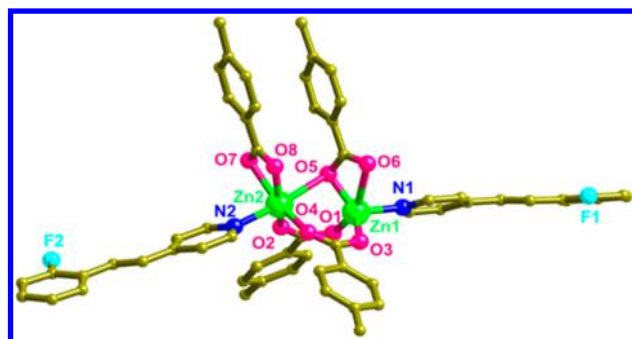


Figure 3. A view of **4** with selected labeling of atoms. The hydrogen atoms are not shown for clarity.

angle of 24° between the plane containing Zn2, O5, O6, and C43 atoms and toluene ring. Hence, Zn2 adopts a distorted octahedral geometry, while Zn1 has a distorted square-pyramidal coordination geometry with the apical position coordinated by a 2F-4spy ligand. Further, the 2F-4spy bonded to Zn1 is disordered. Two independent orientations were modeled with the occupancy refined to 0.818(5) and 0.182(5). One of the bridging ptol ligands was also disordered.

A crystallographic center of inversion is also present on both sides of the molecule close to the middle of the neighboring 2F-4spy ligands as in **1**. The olefin groups of the 2F-4spy ligands bonded to Zn1 are aligned parallel, separated by 3.74 Å and expected to be photoreactive under UV light. Whereas the adjacent 2F-4spy ligands bonded to the Zn2 atoms are also aligned parallel, they are slip-stacked as in **1**. The C=C bond pairs are separated by 4.92 Å (Figure 4), and hence these pairs are expected to behave very similar to **1**.

The photoreactivity was tested under UV light. The ¹H NMR spectrum was recorded after the powdered **4** was irradiated under UV light for 2 h and dissolved in DMSO-*d*₆. The chemical shifts at 8.35 ppm (pyridyl protons) and 4.72 ppm (cyclobutane protons) show the formation of 50% photoreaction of 2F-4spy in a head-to-tail fashion, which

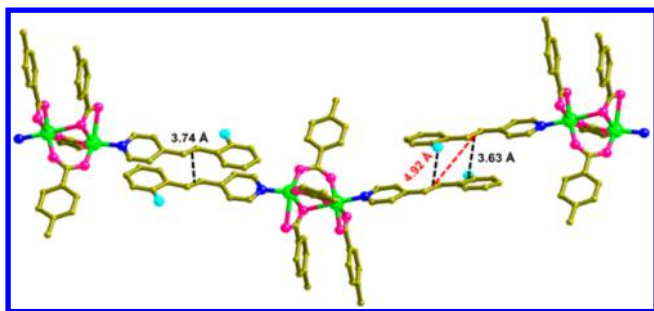


Figure 4. A perspective view of the packing of **4** in the solid state showing how the neighboring 2F-4spy ligands are aligned. The hydrogen atoms are not shown for clarity.

results in the formation of *rctt*-2F-ppcb (*rctt*-2F-ppcb = *rctt*-1,3-bis(4-pyridyl)-2,4-bis(2'-fluorophenyl)cyclobutane), and likely to have originated from the reaction of the ligand bonded to Zn1 atom. In addition to the above peaks, the ^1H NMR spectrum exhibits several new peaks similar to those of UV irradiated powder **1**, which do not belong to either *rctt*-2F-ppcb or 2F-4spy ligands, suggesting that there might be some other photoreaction occurring instead (see below). However, they were poorly resolved to deduce any structural information clearly.

In order to determine the solid-state structure of the unusual photoproduct (**5**) unequivocally by single crystal X-ray diffraction methods, we attempted to retain the single crystals at the end of the UV experiments and eventually succeeded. By virtue of this SCSC transformation, complete solid-state structural elucidation of **5** was possible, and the results are discussed below.

Even after the $[2 + 2]$ photo-cycloaddition reaction, compound **5** exists in the space group $P2_1/c$ as **4**. During the photoreaction, the volume of the cell was reduced by $\sim 2\%$ with changes in the lengths of *a*- and *c*-axes (Supplementary Table 1). As expected from the precursor structure **4**, the aligned C=C bond pairs in 2F-4spy ligand coordinated to Zn1 show quantitative $[2 + 2]$ cycloaddition reaction and resulted in the formation of *rctt*-2F-ppcb. The crystallographic inversion center is still preserved in the photo product on both sides of $\text{Zn}_2(\text{ptol})_4$ core. However, the photo-cycloaddition of 2F-4spy pair which is bonded to Zn2 (where the olefin groups are separated by 4.92 Å) showed disorder marred by the presence of inversion symmetry. Upon further comparison with the structure of **4**, it was realized that the olefin bonds are aligned parallel to the aromatic C–C bonds with a distance of 3.63 Å in a complementary manner as shown in Figure 4.

The disorders of the photoproduct between the Zn2 atoms in **5** could be modeled successfully in two ways in the least-squares refinement cycles: (i) reaction between one olefin bond and a phenyl group yielding bicyclo[4.2.0]octa-2,4-diene derivative (here after called as **L1F**, see Figure 5) which possess a very highly strained bicyclic ring containing four stereocenters in a quantitative yield. The ligand **L1F** is disordered due to crystallographic inversion symmetry. (ii) Both the olefin bonds from the neighboring 2F-4spy ligands reacted with the adjacent phenyl groups to furnish ladderane like structure (here after mentioned as **L2F**, see Figure 5) with five rings fused together along with 50% of the unreacted 2F-4spy ligands.

To determine the correct structure unambiguously between these two possibilities, ^{19}F NMR spectrum of **5** was recorded

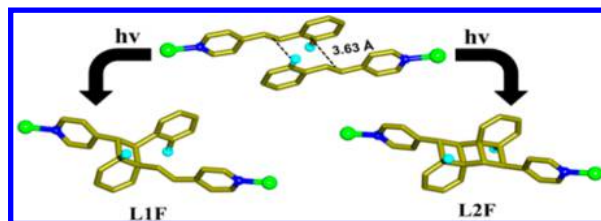


Figure 5. Olefin–phenyl interactions in **4** and the possible photoproducts of UV irradiation experiment of **4**. For clarity the hydrogen atoms are not shown.

and compared with **4** and the *rctt*-2F-ppcb in a metal complex (Figure 6a). The ^{19}F NMR spectra of **4** and *rctt*-2F-ppcb show peaks at -117.7 ppm and -115.9 ppm, respectively, whereas **5** exhibits three peaks, at -110.5 ppm, -114.5 ppm, and -115.9 ppm. The absence of NMR peak at -117.7 ppm confirms that there is no unreacted 2F-4spy ligand in **5**, and the presence of a peak at -115.9 ppm shows the formation of *rctt*-2F-ppcb. Hence, the chemical shifts at -110.5 ppm and -114.5 ppm are

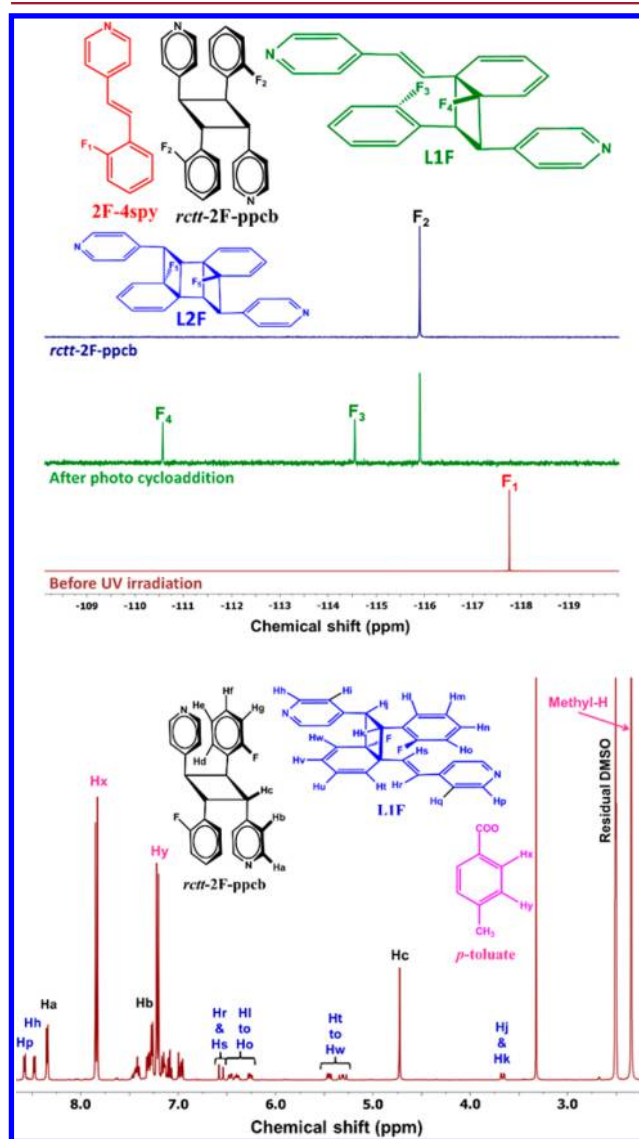


Figure 6. ^{19}F NMR spectra of **4**, **5** and *rctt*-2F-ppcb in a Zn(II) complex (from bottom to top) in $\text{DMSO}-d_6$ (above). The ^1H NMR spectrum of **5** showing the formation of **L1F** (below).

due to either **L1F** or **L2F**. Two different chemical shifts are expected from two different F atoms in **L1F** but not in **L2F**. Further, X-ray structure analysis of **4** indicates that the formation of **L2F** should be accompanied by 50% of the unreacted 2F-4spy ligand. Hence, ^{19}F NMR data clearly confirm the formation of **L1F** over **L2F**. In addition, ^1H NMR spectrum of the photoproduct **5** correlated well with **L1F** structure, but not with **L2F** (Figure 6b, Figure S16 in Supporting Information).

The combination of the crystallographic data along with ^{19}F and ^1H NMR spectral results corroborate the formation of a novel bicyclic product **L1F** through an unprecedented $[2 + 2]$ cycloaddition reaction between an olefin bond and a phenyl ring. The photoreaction of **4** had led to the formation of a 1D coordination polymeric structure, **5** containing both of *rctt*-2F-ppcb and **L1F** alternately between the $\text{Zn}_2(\text{ptol})_4$ cores.

To understand the stability of these highly strained rings, the powdered **5** was heated at $175\text{ }^\circ\text{C}$ for 22 h, and the product was characterized by ^1H NMR spectroscopy (Figure S17 in Supporting Information). Interestingly, it has been found that the **L1F** dissociated back to 2F-4spy, but *rctt*-2F-ppcb was still intact during heating. This suggests that the bicyclic ring **L1F** is relatively unstable and can be thermally cleaved reversibly.

Solid-state $[2 + 2]$ photo-cycloaddition reactions have been investigated extensively, and they occur exclusively between a pair of olefin bonds. Although phenyl–olefin bonds have been found to be closely aligned in the solid state structures, they have been found to be either photoinert or sliding of molecules occurs to favor $[2 + 2]$ cycloaddition reaction between olefins. Such a $[2 + 2]$ cycloaddition reaction between the phenyl and olefin groups encountered here is scarce in the solid state. One such phenyl–olefin reaction has been reported in 66% conversion as characterized by NMR spectroscopy.¹⁵ In this work, although nicely aligned, the reaction between phenyl and olefin bond is very sluggish between 4spy pairs, whereas the reaction is facile when a fluorine is introduced in 4spy. This unusual phenyl–olefin cycloaddition reaction results in the formation of a highly strained bicyclic product at the expense of the aromaticity of the phenyl ring in the solid state. The importance of fluorinated benzene on the dynamics and reactivity in the solid state has also been realized recently in azobenzene isomerization reaction.^{30,31} A pair of pyridyl rings in 2-hydroxyquinoline-4-carboxylate ligand has been found to undergo dimerization during the hydrothermal synthesis of metal–organic frameworks.³² The solution reaction is likely to occur between a pair of olefin bonds in the tautomeric forms of the ligand with the loss of aromaticity, rather than between two aromatic pyridyl groups.

To shed light on the observed unusual $[2 + 2]$ phenyl–olefin photo-cycloaddition reaction, density functional theory (DFT) calculations were performed with the M06-2X functional,³³ using the Gaussian 09 program.³⁴ To elucidate the π – π stacking interaction between two 4spy ligands in crystals **1** and **4**, the binding energies of a pair of 4spy and a pair of 2F-4spy in both X-ray structures were evaluated at M06-2X/6-311+G-(2df,p) + BSSE level. The π -stacking stabilization energies of both types of dimer in two different geometries of stacking arrangement, namely, face-to-face and displaced parallel, are fairly large, between -29 and -35 kJ mol^{-1} (Figure S24 in Supporting Information). In both cases, fluoro substitution leads to a slight increase in interaction energy, by 3 – 5 kJ mol^{-1} . Interestingly, full geometry optimizations of a pair of free 2F-4spy dimers yield geometries fairly close to the observed ligand

pair geometries in the crystal (Figure S25 in Supporting Information). These results clearly indicate that the π – π stacking interaction between 4spy moieties plays an essential role in the crystal packing of **1** and **4**. The enhanced stability of the 2F-4spy dimers is attributed to the direct electrostatic interaction between the fluoro substituent and the adjacent phenyl ring.³⁵

The experimental and theoretical studies of benzene/phenyl ring activation in solution using UV light to S_1 excited state has been reported in the literature.^{18,36–38} We calculated the HOMO of the lowest excited state using the TD-DFT method^{39,40} at the M06-2X/6-31+G* level, to further investigate this novel solid-state photoreaction. As expected, the HOMO of the excited states has a major contribution from the ethylene moiety (Figure 7), which can react with another

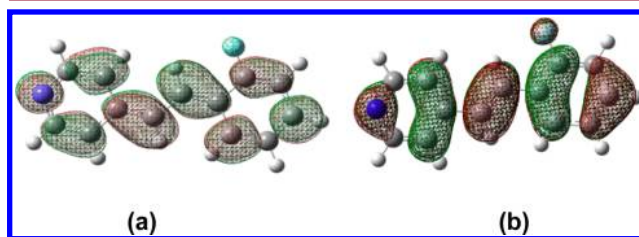


Figure 7. (a) HOMO of the lowest excited singlet state of 2F-4spy. (b) HOMO of the ground state of 2F-4spy. Note the change of HOMO orbital symmetry from symmetric in the ground state to antisymmetric in the excited state for the two carbon atoms of fluorophenyl moiety that forms cyclobutane of **L1F**.

alkene to give cyclobutane when the two olefin units are aligned properly within the Schmidt's radius. Furthermore, there is a smaller but significant orbital contribution from the phenyl moiety (Figure 7). Most importantly, the required antisymmetric symmetry is satisfied at the C–C bond indicated for $[2 + 2]$ phenyl–olefin cycloaddition. Thus, our MO calculations confirm that the phenyl–olefin photo-cycloaddition is symmetry allowed.

Structural analysis of the excited singlet state geometries of 4spy and 2F-4spy indicates that the aromaticity of the phenyl ring is reduced in both cases and to a greater extent in 2F-4spy, as evidenced from the larger deviation of C–C bond lengths in 2F-4spy (Figure S26 in Supporting Information). This is evidently a result of the participation of the p_z orbital of the 2-fluoro substituent in the π conjugation. As a consequence of the loss of aromaticity of the phenyl ring by photo excitation, the excited system is more susceptible to cycloaddition with olefins, when the desired overlap at the ethylene moiety with another ground state double bond is not available in the solid state. The greater reduction of aromaticity of 2F-4spy in the excited singlet state compared to the 4spy system may explain the observed reactivity difference between the two systems. The improved reactivity in 2F-4spy may also be attributed to the fact that the phenyl–olefin distance is shorter in 2F-4spy than 4spy (3.63 versus 3.69 \AA).

Dewar benzene is an interesting isomer of benzene that has two highly strained nonconjugated double bonds.⁴¹ Hence, a conceivable alternate reaction pathway for the formation of **L1F** would involve one 2F-4spy isomerizing to a Dewar-benzene isomer, followed by $[2 + 2]$ cycloaddition to the ethylene moiety of another 2F-4spy. For 2F-4spy, such a Dewar-benzene isomer (Figure S27 in Supporting Information) is substantially higher in energy, by 307.2 kJ mol^{-1} , and the optimized

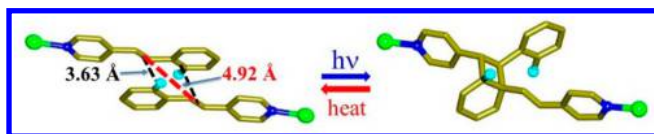
geometry is strongly distorted from the planar geometry (Figure S27 in Supporting Information). Therefore, based on reaction thermodynamics and crystal packing considerations, it is less likely that the observed $[2 + 2]$ cycloaddition occurs via a Dewar-benzene intermediate.

It is intriguing to observe that a second $[2 + 2]$ phenyl–olefin cycloaddition from **L1F** to yield **L2F** does not occur. This can be explained by the fact that the conjugation which enables activation of phenyl in 2F-4spy no longer exists upon formation of **L1F** together with the increase in the distance between the phenyl and olefin group after cyclobutane formation. The nonconjugated fluorophenyl group is expected to undergo photo excitation at wavelength significantly less than 320–360 nm. This hypothesis is readily supported by TD-DFT calculations of **L1F** and 2F-4spy (Supplementary Table 2). The lowest UV absorption wavelength with significant oscillator strength of **L1F** is shorter by 32 nm compared to that of 2F-4spy.

CONCLUSION

In summary, we observed an unusual solid-state $[2 + 2]$ cycloaddition reaction between a phenyl ring and an olefin group along with the expected usual photodimerization reaction between a pair of olefin bonds in a Zn(II) complex containing 2F-4spy ligand (as shown in Scheme 2). The

Scheme 2. Solid State $[2 + 2]$ Photo-Cycloaddition Reaction between Phenyl–Olefin Bonds and Its Reversible Reaction of Cleavage of the Cyclobutane Ring by Heating



formation of a rare bicyclic product, **L1F** has been confirmed by single crystal X-ray diffraction experiments due to SCSC reaction, in conjunction with ^1H NMR and ^{19}F NMR studies. Thus, this solid-state reaction paved the way for accessing highly strained bicyclic compounds easily in quantitative yield. This unique reaction has been observed exclusively when 2F-4spy was used in **4**. In a similar packing, 4spy pair in **1** does not undergo phenyl–olefin cycloaddition reaction readily, although methyl groups of the toluate ligands enforced such interaction to be robust in single crystals. In both cases, the end product is expected to be 1D coordination polymers. But in the case of **5**, the $\text{Zn}_2(\text{ptol})_4$ core is connected with two different types of photoproducts.

It appears that the fluorine substitution is needed for the activation of the reaction between the phenyl and olefin groups. Thus, in addition to crystal engineering of reactive bonds, reaction engineering has also been accomplished successfully in the solid state by fluorine substitution. These results observed here hope to engineer the ubiquitously observed phenyl–olefin interactions to undergo $[2 + 2]$ cycloaddition reaction in the solid state for making new and potentially useful bicyclic derivatives.

ASSOCIATED CONTENT

Supporting Information

Experimental procedures, ^1H NMR, PXRD, and TG analysis and other computational details are included in the Supporting Information. The Supporting Information is available free of

charge on the ACS Publications website at DOI: 10.1021/acs.cgd.5b00664.

AUTHOR INFORMATION

Corresponding Authors

*E-mail: chmwmw@nus.edu.sg.

*E-mail: chmjv@nus.edu.sg.

Notes

The authors declare no competing financial interest.

ACKNOWLEDGMENTS

We thank the Ministry of Education, Singapore for financial support through NUS FRC Grant Nos. R-143-000-562-112 and R-143-000-604-112, (Late) Prof. Lip Lin Koh, Ms. Geok Kheng Tan and Ms. Yimain Hong for their help in X-ray data collection.

REFERENCES

- (1) Liebermann, C.; Bergami, O. *Ber. Dtsch. Chem. Ges.* **1889**, *22*, 782.
- (2) Bernstein, H. I.; Quimby, W. C. *J. Am. Chem. Soc.* **1943**, *65*, 1845.
- (3) Cohen, M. D.; Schmidt, G. M. J. *J. Chem. Soc.* **1964**, 1996.
- (4) Schmidt, G. M. J. *Pure Appl. Chem.* **1971**, *27*, 647.
- (5) Cohen, M. D.; Schmidt, G. M. J.; Sonntag, F. I. *J. Chem. Soc.* **1964**, 2000.
- (6) Theocharis, C. R.; Jones, W. In *Organic Solid State Chemistry*; Desiraju, G. R., Ed.; Elsevier: Amsterdam, 1987; p 47.
- (7) Ramamurthy, V.; Venkatesan, K. *Chem. Rev.* **1987**, *87*, 433.
- (8) Green, B. S.; Lahav, M.; Rabinovich, D. *Acc. Chem. Res.* **1979**, *12*, 191.
- (9) Jones, W. *Organic Molecular Solids: Properties and Applications*; CRC Press: Boca Raton, FL, 1997.
- (10) Kaupp, G.; Naimi-Jamal, M. R. *CrystEngComm* **2005**, *7*, 402.
- (11) Kaupp, G. In *Organic Solid State Reactions*; Toda, F., Ed.; Springer: Berlin, 2005; Vol. 254, p 95.
- (12) Harada, J.; Ogawa, K. *Chem. Soc. Rev.* **2009**, *38*, 2244.
- (13) Kole, G. K.; Vittal, J. J. *Chem. Soc. Rev.* **2013**, *42*, 1755.
- (14) Thomas, I. R.; Bruno, I. J.; Cole, J. C.; Macrae, C. F.; Pidcock, E.; Wood, P. A. *J. Appl. Crystallogr.* **2010**, *43*, 362.
- (15) Ito, Y.; Horie, S.; Shindo, Y. *Org. Lett.* **2001**, *3*, 2411.
- (16) Bach, T.; Hehn, J. P. *Angew. Chem., Int. Ed.* **2011**, *50*, 1000.
- (17) Alonso, R.; Bach, T. *Angew. Chem., Int. Ed.* **2014**, *53*, 4368.
- (18) Hoffmann, N. *Synthesis* **2004**, *4*, 481.
- (19) Horwitz, L. *J. Org. Chem.* **1956**, *21*, 1039.
- (20) Williams, J. L. R.; Adel, R. E.; Carlson, J. M.; Reynolds, G. A.; Borden, D. G.; Ford, J. A. *J. Org. Chem.* **1963**, *28*, 387.
- (21) Bučar, D.-K.; MacGillivray, L. R. *J. Am. Chem. Soc.* **2007**, *129*, 32.
- (22) Takahashi, S.; Miura, H.; Kasai, H.; Okada, S.; Oikawa, H.; Nakanishi, H. *J. Am. Chem. Soc.* **2002**, *124*, 10944.
- (23) Karunatilaka, C.; Bučar, D.-K.; Ditzler, L. R.; Friščić, T.; Swenson, D. C.; MacGillivray, L. R.; Tivanski, A. V. *Angew. Chem., Int. Ed.* **2011**, *50*, 8642.
- (24) Al-Kaysi, R. O.; Müller, A. M.; Bardeen, C. J. *J. Am. Chem. Soc.* **2006**, *128*, 15938.
- (25) Sheldrick, G. M., University of Göttingen, Germany, 1996.
- (26) Sheldrick, G. M. *Acta Crystallogr., Sect. A* **2008**, *64*, 112.
- (27) Müller, P.; Herbst-Irmer, R.; Spek, A.; Schneider, T.; Sawaya, M. *Crystal Structure Refinement: A Crystallographer's Guide to SHELXL*; Oxford University Press: Oxford, U.K., 2006.
- (28) Hokelek, T.; Ermis, E.; Tercan, B.; Cimen, E.; Necfoglul, H. *Acta Crystallogr., Sect. E* **2010**, *66*, m841.
- (29) Cohen, M. D. *Angew. Chem., Int. Ed. Engl.* **1975**, *14*, 386.
- (30) Bléger, D.; Schwarz, J.; Brouwer, A. M.; Hecht, S. *J. Am. Chem. Soc.* **2012**, *134*, 20597.
- (31) Bushuyev, O. S.; Tomberg, A.; Friščić, T.; Barrett, C. J. *J. Am. Chem. Soc.* **2013**, *135*, 12556.

- (32) Qin, J.; Qin, N.; Geng, C.-H.; Ma, J.-P.; Liu, Q.-K.; Wu, D.; Zhao, C.-W.; Dong, Y.-B. *CrystEngComm* **2012**, *14*, 8499.
- (33) Zhao, Y.; Truhlar, D. *Theor. Chem. Acc.* **2008**, *120*, 215.
- (34) Frisch, M. J., et al. *Gaussian 09*, Revision A.02; Gaussian, Inc., Wallingford, CT.
- (35) Wheeler, S. E.; Houk, K. N. *J. Am. Chem. Soc.* **2008**, *130*, 10854.
- (36) Clifford, S.; Bearpark, M. J.; Bernardi, F.; Olivucci, M.; Robb, M. A.; Smith, B. R. *J. Am. Chem. Soc.* **1996**, *118*, 7353.
- (37) Houk, K. N. *Pure Appl. Chem.* **1982**, *54*, 1633.
- (38) Cornélisse, J. *Chem. Rev.* **1993**, *93*, 615.
- (39) Bauernschmitt, R.; Ahlrichs, R. *Chem. Phys. Lett.* **1996**, *256*, 454.
- (40) Casida, M. E.; Jamorski, C.; Casida, K. C.; Salahub, D. R. *J. Chem. Phys.* **1998**, *108*, 4439.
- (41) Van Tamelen, E. E. *Acc. Chem. Res.* **1972**, *5*, 186.